ukahara S, Ezawa N, Yamanouchi K. 2003. Neonatal estrogen decreases neural density of the septum-midbrain central gray connection underlying the lordosis-inhibiting system in female rats. Neuroendocrinology 78:226–233.

ieyama C, Shibutani M, Masutomi N, Takagi H, Hirose M. 2002. Methacarn fixation for genomic DNA analysis in microdissected, paraffin-embedded tissue specimens. J Histochem Cytochem 50:1237–1245.

ano T, Saito T, Tsukui T, Fujita M, Hosoi T, Muramatsu M, Ouchi Y, et al. 2002. Efp targets 14-3-3σ for proteolysis and promotes breast tumour growth. Nature 417: 871–875.

Wolf CJ, LeBlanc GA, Gray LE Jr. 2004. Interactive effects of vinclozolin and testosterone propionate on pregnancy and sexual differentiation of the male and female SD rat. Toxicol Sci 78:135–143.

Xie T, Tong L, McCann UD, Yuan J, Becker KG, Mechan AO, Cheadle C, et al. 2004. Identification and characterization of metallothionein-1 and -2 gene expression in the context of (±)3, 4-methylenedioxymethamphetamine-induced toxicity to brain dopaminergic neurons. J Neurosci 24:7043–7050.

Available online at www.sciencedirect.com

ScienceDirect

Biochemical and Biophysical Research Communications 365 (2008) 562–567

BBRC

www.elsevier.com/locate/ybbrc

Inducibility of cytochrome P450 1A1 and chemical carcinogenesis by benzo[*a*]pyrene in AhR repressor-deficient mice

Tomonori Hosoya [a,c,1], Nobuhiko Harada [a,b,1], Junsei Mimura [a,d], Hozumi Motohashi [a,b], Satoru Takahashi [b], Osamu Nakajima [a], Masanobu Morita [a], Shimako Kawauchi [a], Masayuki Yamamoto [a,b,c], Yoshiaki Fujii-Kuriyama [a,d,*]

[a] *Center for Tsukuba Advanced Research Alliance, University of Tsukuba, 1-1-1 Tennodai, Tsukuba 305-8577, Japan*
[b] *Graduate School of Comprehensive Human Science, University of Tsukuba, 1-1-1 Tennodai, Tsukuba 305-8577, Japan*
[c] *Exploratory Research for Advanced Technology, Japan Science and Technology Agency, 4-1-8 Honcho, Kawaguchi, Saitama 332-0012, Japan*
[d] *Solution Oriented Research for Science and Technology, Japan Science and Technology Agency, 4-1-8 Honcho, Kawaguchi, Saitama 332-0012, Japan*

Received 30 October 2007
Available online 20 November 2007

Abstract

AhR repressor (AhRR) is an AhR-related bHLH-PAS transcription factor. It is known to repress AhR transcription activity in a competitive manner. To examine AhRR functions in mice, we produced AhRR-deficient mice by gene knockout. *AhRR(−/−)* mice were born in normal Mendelian proportions, grew well, and were fertile. *AhR(−/−)* mice exhibited higher levels of *Cyp1a1* (Cytochrome P450 1A1) mRNA induction in the skin, stomach and spleen than wild-type mice, while expression of *Cyp1a1* mRNA was not significantly altered in the liver, lung, heart or other tissues, suggesting that "super-induction" of *Cyp1a1* mRNA expression in *AhRR(−/−)* mice occurs in a tissue specific manner. *AhRR(−/−)* mice displayed a delayed response to skin carcinogenesis caused by benzo[*a*]pyrene. Since CYP1A1 is involved in the metabolic activation and detoxification of chemical carcinogens, these results suggest that overexpression of CYP1A1 shifts the balance of the metabolic activities in the skin of *AhRR(−/−)* mice in favor of the detoxification of carcinogens.

Keywords: AhR receptor; Gene targeting; Chemical carcinogenesis; CYP1A1; AhR; Transcription; Metabolic activation; Polyaromatic hydrocarbon; Super-induction; Transcription repression

Aryl hydrocarbon receptor (AhR) is a ligand-activated transcription factor belonging to the bHLH (basic helix-loop-helix)-PAS (Per-Arnt-Sim homology) superfamily [1–3]. Normally, AhR exists in the cytoplasm in association with the HSP90 complex. Upon binding with its ligands, such as 3MC (3-methylcholanthrene) and TCDD (2′,3′,7′,8′-tetrachlorodibenzo-*p*-dioxin), AhR translocates to the nucleus, where it heterodimerizes with Arnt (AhR nuclear translocator, another member of the bHLH-PAS superfamily) to induce the expression of a battery of drug-metabolizing enzymes including CYP1A1, 1B1 and 1A2 [1–3]. In addition, recently, the target genes of AhR have been expanded to those involved in cell cycle regulation, apoptosis, endocrine regulation and the immune system [4,5]. Among them, AhRR is unique, because it represses the transcriptional activity of AhR and thus forms a negative feedback regulatory loop in the xenobiotic signal tranduction pathway [6,7]. AhRR (AhR repressor) which was originally identified in mice, has also been reported in many animal species including human [8], rat [9] and fish [10]. In cell culture, AhRR inhibits AhR transcription activity by competing with AhR for heterodimer formation with Arnt; the AhRR/Arnt heterodimer then competes with AhR/Arnt heterodimer for binding to xeno-

* Corresponding author. Address: Center for Tsukuba Advanced Research Alliance, University of Tsukuba, 1-1-1 Tennodai, Tsukuba 305-8577, Japan. Fax: +81 29 853 7318.
E-mail address: ykfujii@tara.tsukuba.ac.jp (Y. Fujii-Kuriyama).
[1] These authors contributed equally to this work.

0006-291X/$ - see front matter © 2007 Elsevier Inc. All rights reserved.
doi:10.1016/j.bbrc.2007.11.016

biotic response element (XRE) sequences [6]. Little is known, however, about the functional role of AhRR in the AhR signaling pathway in living animals.

To investigate the functional roles of AhRR in the AhR signaling system *in vivo*, we generated *AhRR(−/−)* mice by homologous recombination. *AhRR(−/−)* mice were born in normal Mendelian propotions, grew well, and were fertile. We found that *AhRR(−/−)* mice were relatively resistant to skin carcinogenesis induced by benzo[*a*]pyrene (B[*a*]P), compared with the wild type (WT). Skin fibroblast cells derived from *AhRR(−/−)* mice showed a remarkably higher level of *Cyp1a1* mRNA induction in response to B[*a*]P than WT counterparts. This "super-induction" of *Cyp1a1* mRNA was not observed in all the tissues examined of *AhRR(−/−)* mice, indicating that AhRR works as repressor of AhR only in specific tissues.

Materials and methods

Generation of AhRR-deficient mice. We disrupted the AhRR gene in mouse embryonic stem cells as described [11]. A targeting vector was constructed by replacing a part of the 2nd exon and the 2nd intron of the *AhRR* gene with the *NLS-LacZ-neo'* gene cassette as shown in Fig. 1A. The HSV-TK gene was used for negative selection. The linearized targeting vector was electroporated into E14 ES cells, and the cells were subjected to double selection with G418 (0.3 mg/ml) and gancyclovir (2 μM). Double-resistant ES clones were then screened by PCR using a pair of oligonucleotide primers corresponding to the neomycin resistance gene (TV-neo; 5′-TCA GAG CAG CCG ATT GTC TGT TGT GCC CAG TCA T-3′) and *AhRR* gene (AhRR TV-PCR2-2; 5′-AGA CCT GAG AGG TCT AGA CTT GGA TGC TAC-3′) depicted in Fig. 1A as arrowheads. To confirm the homologous recombination, ES clone genomic DNA was digested with PstI or BamHI restriction enzymes for DNA blot analysis using 5′ or 3′ external probes. Positive ES clones were injected into blastocoel cavities of 3.5-day postcoitum (dpc) blastocysts derived from C57BL/6 mice. The injected blastocysts were surgically transplanted into the uteri of pseudo-pregnant ICR recipient mice at 2.5 dpc. Germ-line transmission of the *AhRR* defective allele was screened by PCR to obtain two independently targeted founder mice, and heterozygous F1 mice were intercrossed to obtain *AhRR(−/−)* mice. Tail DNAs of the pups were extracted and subjected to PCR for the presence of the mutated *AhRR* allele using the TV-neo and AhRR TV-PCR2-2 primers. To distinguish easily the mutated *AhRR* alleles from WT by PCR, the following oligonucleotides were used as PCR primers: AhRR KO-5′ (5′-GAA ACT GTA GCC CTG GAT ACT TCT G-3′), AhRR KO-3′ (5′-ATC ATT GCT CTG AGC ATC CAC TAG G-3′) and TV neo primer. The AhRR KO-5′ and 3′ primer pair amplifies only the *AhRR* wild-type allele (190 bp), while that of the AhRR KO-3′ and TV neo primers amplifies only the mutated one (527 bp).

PCR-RFLP analysis. Because the established *AhRR* mutant mice contain both C57BL/6 and 129Sv *AhR* alleles, PCR-restriction fragment length polymorphism (RFLP) analysis was performed to exclude the 129Sv *AhR* allele, as described [8,12]. Briefly, tail genomic DNAs were amplified by PCR with a primers OL72 (5′-GGT TCG AAT TTC CAG GAT GG-3′) and OL111 (5′-CCA CCC CAG GTA CAT GAT GGA ACC-3′). PCR fragments were digested with *Eco47*III restriction enzyme and electrophoresed on an 8.0% acrylamide gel. The C57BL/6 *AhR* allele yields 142 and 76 bp fragments, while the 129Sv *AhR* allele yields a 218 bp fragment. Mice homozygous for the C57BL/6 *AhR* allele were used for further analyses.

Chemical treatment and tumor induction. B[*a*]P and 3MC were obtained from Wako Junyaku Co. (Osaka). To analyze *Cyp1a1* induction in mouse tissues, corn oil (vehicle control) or 3MC dissolved in corn oil (4 mg/ml) was intraperitoneally injected into mice (80 mg/kg body weight), and the mice were sacrificed 24 or 48 h after injection. Tissues were collected from the mice and subjected to RNA extraction for RT-PCR analysis, as described [6]. For tumor induction experiments, *AhRR(−/−)* mice were backcrossed with wild-type C57BL/6 mice for at least 7 generations, and subcutaneously injected with 0.2 ml of B[*a*]P in corn oil (10 mg/ml) twice, a week apart, as described [13]. All mice of 8 weeks of age were examined for development of tumors at least once a week for 30 weeks until death. The tumor sizes were recorded throughout the experimental period. Tumor-bearing mice were counted and presented as percentage of the total. Tumors were dissected, fixed in formalin and embedded in paraffin. Sections at 3-μm thickness were stained with hematoxylin and eosin as described previously [14].

Skin fibroblast cell culture preparation. WT and *AhRR(−/−)* skin fibroblast cultures were prepared from the skin of at least six neonatal mice, respectively. Skin was removed from newborn mice, and then minced into small pieces, followed by digestion with 1% collagenase (SIGMA) in DMEM for 1 h at 37 °C. The digests were then rinsed once with PBS, then maintained in DMEM supplemented with 10% FBS and penicillin/streptomycin at 37 °C in 5% CO_2 until skin fibroblast cells covered the entire culture dish plate. The cells were replated at 2.0×10^6 cells per 10 cm diameter dish for further experiments and passage.

Cell treatments and RT-PCR. Skin fibroblast cell cultures were incubated in the absence (DMSO) or presence of 1 μM B[*a*]P (DMSO solution) as described in figure legends. Total RNA was extracted from the cells with TRIsure RNA extraction reagent and reverse-transcribed into cDNA by using SuperScript II RTase. Quantitative gene expression analysis was

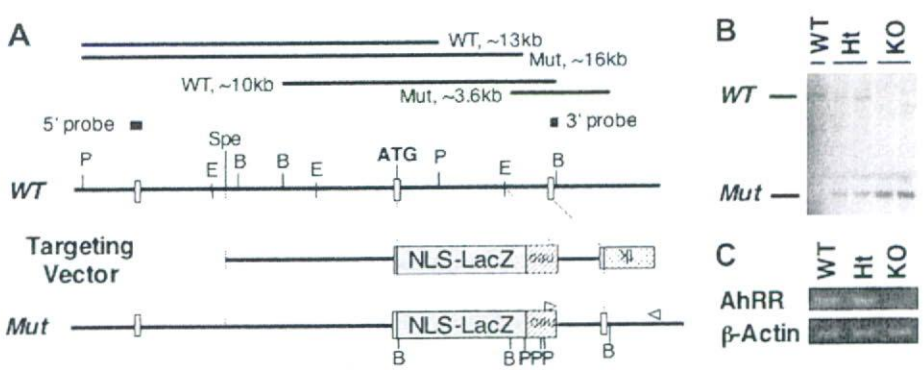

Fig. 1. Targeted disruption of the mouse *AhRR* gene. (A) Schematic representation of the targeting vector, *AhRR*-WT and Mut alleles. Cleavage sites for the restriction enzymes are indicated by E (EcoRI), B (BamHI), Sp (SpeI) and P (PstI). The locations of the 5′ and 3′ probes used for the DNA blot analysis are indicated at the top. Two arrowheads indicate the position of primers used to identify homologous recombinant clones. (B) DNA blot of mouse genome using the 3′ probe. Genomic DNA (10 μg) was digested with BamHI; digested products were then electrophoresed and hybridized. (C) Mice were treated with 3MC for 24 h, and then total RNA from spleen was subjected to RT-PCR analysis.

performed by using Platinum SYBRGreen qPCR premix in an ABI7300 qPCR analyzer. PCR primers for CYP1A1: 5′-GGACATTTGAGAA GGGCCAC-3′ and 5′-CGTCCAGCTTCCTGTCCTGA-3′; for CYP1B1: 5′-GGATGTGCCTGCCACTATTAC-3′, 5′-CCTGAACATCCGGGTA TCTG-3′; for AhRR; 5′-CCTGTCCCGGGATCAAAGATG-3′ and 5′-CTCACCACCAGAGCGAAGCCATTGA-3′; for β-actin: 5′-GTGAAA AGATGACCCAGATCATG-3′ and 5′-GTGGTACGACCAGAGGCA TAC-3′.

β-Galactosidase staining. Tissues were fixed overnight in PBS containing 4% paraformaldehyde, dehydrated with ethanol, embedded in paraffin and sectioned at 3-μm thickness. The sections were dewaxed and stained. β-galactosidase staining was carried out as described [15].

Results

Targeted disruption of mouse AhRR gene

To investigate the functional role of AhRR *in vivo*, we generated an *AhRR* knockout mouse by gene targeting technology as described [15]. The *NLS-LacZ* sequence was fused in a reading frame with the 8th amino acid of the *AhRR* gene so that the inserted *NLS-LacZ* gene could mimic the mode of *AhRR* gene expression (Fig. 1A). Since the resulting protein product lacks most of the coding region of the bHLH domain, which is essential for dimerization and DNA binding, we expected that the knockout mice would lack AhRR function. E14 embryonic stem (ES) cells were electroporated with the linearized targeting vector and subjected to positive-negative selection. Of the 360 clones screened by PCR, nine clones had undergone homologous recombination at the *AhRR* locus, as subsequently confirmed by DNA blot (Fig. 1B). The mutant clones were proliferated and microinjected into C57BL/6 recipient blastocysts to generate chimeric mice, and the male chimeras were crossed with C57BL/6 females. Ultimately, two independent mutant ES cells were successfully transmitted to offspring.

Generation of homozygous AhRR mutant mice

AhRR(+/−) mutant mice were viable and fertile, and were intercrossed for analysis of the phenotypes of *AhRR(−/−)* homozygosity. Offspring of all three genotypes were born at a normal Mendelian proportion in both mixed and C57BL/6 backgrounds (Table 1).

To assess complete inactivation of the gene, the absence of *AhRR* mRNA was confirmed by RT-PCR. Intraperitoneal injection of 3MC induced *AhRR* mRNA expression in the heart of wild-type and *AhRR(+/−)* mice, whereas *AhRR* mRNA was not found in the *AhRR(−/−)* (Fig. 1C). Taken together with the results of the DNA blots (Fig. 1B), these results confirmed the specific disruption of the *AhRR* gene.

Table 1
Genotypes of offspring obtained by double heterozygous mating

Background[a]	WT	Ht	KO	*n*
Mix	63 (20.3%)	166 (53.4%)	**82** (26.4%)	311
B6	30 (30.6%)	49 (50.0%)	**19** (19.4%)	98

[a] Mating was performed with heterozygous mice in C57BL/6 and 129SV background (Mix) or mice backcrossed to C57BL/6 background 7 generations (B6).

The general behaviors including feeding, growth and mating of AhRR*(−/−)* mice were apparently normal, and the mutants lived a normal lifespan (data not shown). Gross anatomy did not reveal any anomaly in AhR*(−/−)* mice.

Gene expression in AhRR(−/−) mice

To investigate the repressor function of AhRR *in vivo*, 3MC was intraperitoneally injected into *AhRR(−/−)* and WT mice. After 24 h of treatment, expression levels of *Cyp1a1* mRNA, one of the well-known AhR target gene products, were measured in various tissues along with the levels of *AhRR* mRNA (Fig. 2A). As previously observed [6], in WT mice, *AhRR* mRNA was highly induced by 3MC in heart, lung, and spleen, and weakly in liver, kidney, thymus intestine, brain and stomach. On the other hand, *Cyp1a1* mRNA was highly induced in lung, liver and heart in WT mice, while this high induction was not much affected in the same tissues of *AhRR(−/−)* mice. In spleen and stomach, induction level of *Cyp1a1* mRNA was higher in *AhRR(−/−)* mice than in WT. The higher induction of *Cyp1a1* mRNA in *AhRR(−/−)* than in WT mice was not observed in all the tissues examined, i.e., induction was tissue-dependent.

We performed a time-course study of *Cyp1a1* mRNA expression in the 3MC-injected mouse spleen (Fig. 2B). In WT mice, *Cyp1a1* mRNA was gradually increased and reached a plateau at 48 h after the 3MC injection. In contrast, in *AhRR(−/−)* mice, *Cyp1a1* mRNA continued to increase to a higher level than in WT mice throughout the course of the experiment. These results support the idea that AhRR represses AhR activity in WT mice.

In addition to spleen and stomach, 3MC treatment also induced the expression of *Cyp1a1* mRNA in the skin of *AhRR(−/−)* mice to a higher level than in WT skin (Fig. 2C).

Because both *AhR* [12] and *AhRR* disrupted genes were inserted in a reading frame of the respective genes with NLS-*LacZ*, we were able to examine the expression patterns of AhR and AhRR in the skin by β-galactosidase staining. AhRR expression was restricted to the dermal fibroblasts (Fig. 3A and C), while AhR was expressed in both fibroblasts and epidermal cells (Fig. 3B and D). To investigate the expression of AhRR and CYP1A1 in the dermal fibroblasts in detail, we isolated dermal fibroblasts from *AhRR(−/−)* and WT mice, and cultured them for treatment with B[*a*]P. *AhRR* mRNA was clearly induced in response to B[*a*]P in WT fibroblasts (Fig. 3E), whereas no expression of AhRR was observed in *AhRR(−/−)* cells. On the other hand, *AhRR(−/−)* fibroblast cells induced *Cyp1a1* mRNA in response to B[*a*]P to a level much higher

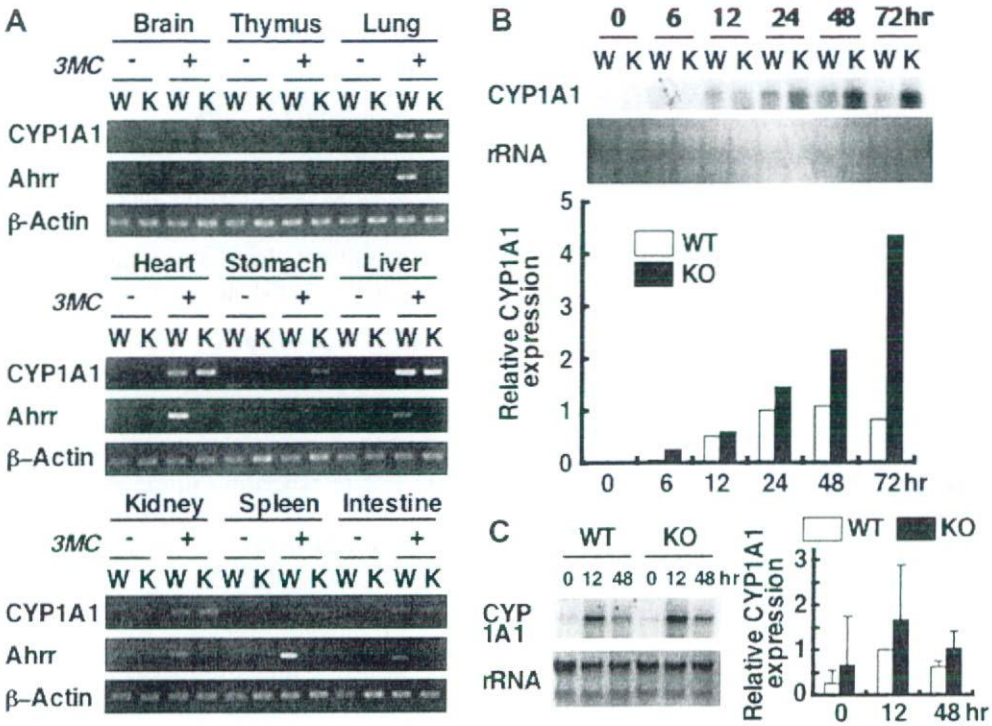

Fig. 2. Inducibility of *AhRR* and *Cyp1a1* mRNA in various tissues. (A) Expression of *Cyp1a1* and *AhRR* mRNA in various tissues of wild type (W) and *AhRR(−/−)* (K) mice. The mice were intraperitoneally injected with 3MC (80 mg/kg body weight). After 24 h, *Cyp1a1* and *AhRR* mRNA expression levels were examined by RT-PCR. Expression levels were normalized on the basis of β-actin expression. (B) A time course of *Cyp1a1* mRNA expression in spleen of wild-type (W) and *AhRR(−/−)* (K) mice after 3MC treatment. Wild-type or *AhRR(−/−)* mice were treated with 3MC; at indicated times after the treatment, RNA was extracted from spleen of the 3MC-treated mice and *Cyp1a1* mRNA expression was examined by RNA blot. *Cyp1a1* mRNA levels are presented relative to the wild-type value at 24 h. (C) Induction of *Cyp1a1* mRNA in skin of wild-type (WT) and *AhRR(−/−)* (KO) mice. 3MC was intraperitoneally injected into wild-type or *AhRR(−/−)* mice. RNA was extracted from the skin of the treated mice and used for determination of *Cyp1a1* mRNA by RNA blot. Average values of the four mice for each group are presented relative to the wild type at 12 h, with standard deviation.

than the wild type, and the induction continued to increase throughout the 24 h experiment. In contrast, wild-type cells slightly increased *Cyp1a1* mRNA but had decreased its expression by 24 h after the treatment. This "super-induction" of CYP1A1 in *AhRR(−/−)* skin fibroblast cells clearly suggest that AhRR works as a negative regulator of CYP1A1 in skin fibroblasts.

Skin carcinogenesis induced by B[a]P in AhRR KO mice

It is known that AhR mediates B[*a*]P carcinogenicity in the skin through expression of CYP1A1 [14]. We wished to investigate the carcinogenicity of B[*a*]P in the skin of *AhRR(−/−)* mice. Both *AhRR(−/−)* and WT mice were injected with B[*a*]P subcutaneously twice, a week apart, and the generation of skin carcinomas was observed thereafter (Fig. 4A). In WT mice, the first subcutaneous tumor was observed 12 weeks after the first treatment of B[*a*]P, and all the mice bore skin tumors 25 weeks after the treatment. On the other hand, the incidence of skin tumors in *AhRR(−/−)* mice was significantly delayed, ~5 weeks behind WT mice. Since CYP1A1 is known to be involved in both metabolic activation and detoxification of chemical carcinogens [16], these results suggest that overexpression of CYP1A1 shifts the balance of metabolic activity of *AhRR(−/−)* skin fibroblasts in favor of detoxification. Histological analysis of the tumors revealed that they were mostly fibrosarcomas, with a minor population of rhabdomyosarcomas and squamous cell carcinomas (data not shown), consistent with a previous report [14]. WT mice showed a slightly higher mortality than *AhRR(−/−)*, but without statistical significance (Fig. 4B).

Discussion

Previously, we reported that AhRR functions as a repressor of the AhR activity, based on transient DNA transfection experiments using cultured cell lines. AhRR represses the transactivation activity of AhR by competing with AhR for heterodimer formation with Arnt; the Arnt-AhRR heterodimer then competes for binding to XRE sequences [6]. To investigate the physiological roles of AhRR *in vivo*, we generated *AhRR(−/−)* mice by homologous gene recombination. The homozygous *AhRR(−/−)* mice were born at normal Mendelian ratios in genetic cross experiments using heterozygous AhRR mutant female and male mice. Mutants grew well and were fertile, indicating that AhRR is dispensable for mouse development and homeostasis. When given 3MC intraperitoneally as an inducer, *AhRR(−/−)* mice exhibited a higher level of CYP1A1 induction in the spleen, stomach and skin than WT mice. In contrast, CYP1A1 induction was not signifi-

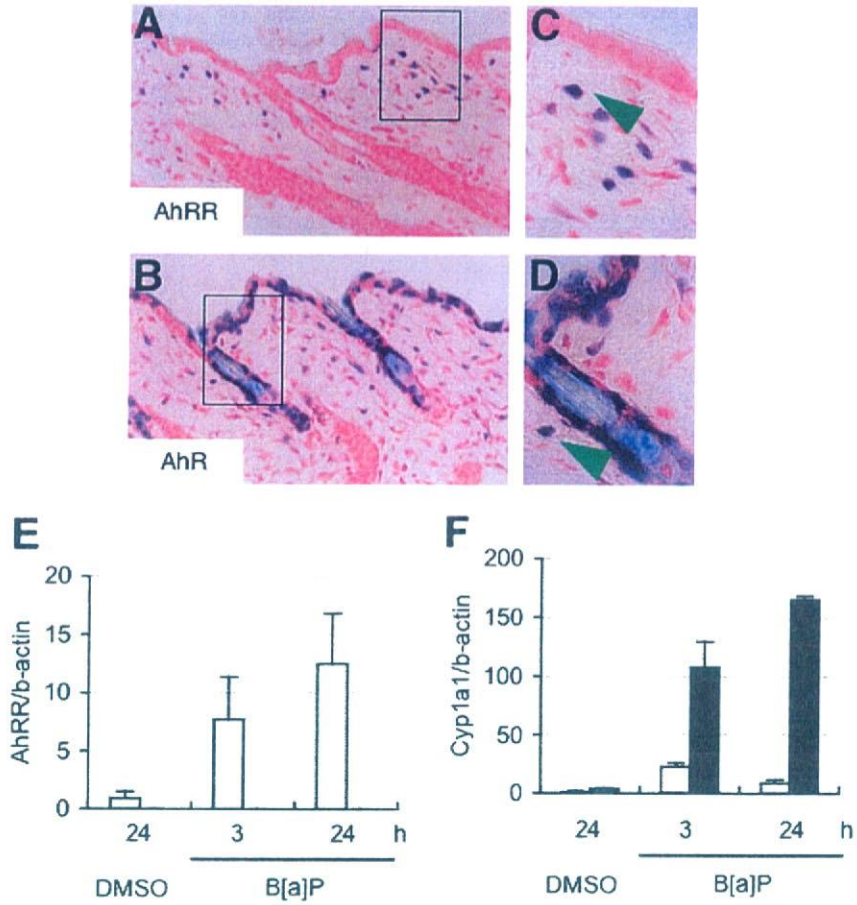

Fig. 3. Cyp1a1 and AhRR expressions in the skin and the skin fibroblast cells of wild-type and *AhRR(−/−)* mice. (A–D) AhRR and AhR expression in the skin. Skin sections prepared from *AhRR(−/−)* (A,C) or *AhR(+/−)* mice (B,D) were subjected to β-galactosidase staining for detection of AhRR or AhR expressing cells. Arrowheads indicate the blue (positive) signal in skin fibroblasts. (E) Expression of *AhRR* mRNA in the isolated skin fibroblast cells of wild-type mice after B[*a*]P treatment. Skin fibroblast cells were treated with vehicle (DMSO) or 1 mM B[*a*]P for 3 and 24 h. Total RNA was extracted from the treated cells and used for quantitation of AhRR by RT-PCR. (F) Expression of *Cyp1a1* mRNA in isolated skin fibroblast cells of wild-type and *AhRR(−/−)* mice after B[*a*]P treatment. Skin fibroblast cells were prepared from wild-type (open bars) and *AhRR(−/−)* mice (closed bars) as described above. The cultured cells were treated with B[*a*]P, and analyzed for *Cyp1a1* mRNA expression by the RT-PCR.

cantly affected in other tissues such as heart and lung, despite high inducibility of *AhRR* mRNA in these tissues of WT mice. Although the reason for this tissue-specific variation of the inducibility of CYP1A1 remains to be investigated, we speculate that protein levels of AhRR may vary from tissue to tissue, probably due either to stability of the protein or translational control. Recently, we have observed that the AhRR protein can undergo modifications, such as ubiquitination and sumoylation has been found to occur (our unpublished observations), and these alterations may be associated with the tissue-specific variation in the inducibility of *Cyp1a1* mRNA expression in *AhRR(−/−)* mice. Investigations of the detailed tissue-specific expression profiles of the AhRR protein are now underway. A study of expression of *LacZ*, which is knocked-in to the *AhR* and *AhRR* loci, revealed that AhR and AhRR are coexpressed in the skin fibroblasts under uninduced conditions. In the heterozygous *AhRR(+/−)* mice skin sections, we could not detect any ß-galactosidase staining, which was observed only in the skin of *AhRR(−/−)* mice (Fig. 3 and data not shown). This is probably because AhRR, which was expressed in *AhRR(+/−)* mice, repressed AhR activity; therefore, AhR-regulated *AhRR* expression was repressed below a detectable level in *AhRR(+/−)* mice. The lack of AhRR expression resulted in the enhancement of AhR activity, leading to the LacZ expression from the *LacZ*-knocked-in *AhRR* gene, in support of the notion that AhRR represses the AhR activity in the skin fibroblasts. These results are confirmed by the experiments using isolated skin fibroblast cells. *AhRR* mRNA was enhanced in WT cells in response to B[*a*]P, together with a slight, but significant enhanced expression of CYP1A1. On the other hand, induction of *Cyp1a1* mRNA was observed in *AhRR(−/−)* skin fibroblasts with significantly higher levels than WT.

AhR mediates carcinogenesis caused by chemical carcinogens through expression of CYP1A1 [14,17]. *AhR(−/−)* mice are resistant to chemical carcinogenesis caused by B[*a*]P [14], because they have essentially no expression of CYP1A1. In this report, *AhRR(−/−)* mice were found to be relatively resistant to chemical carcinogenesis induced by B[*a*]P, as compared with WT mice. Since CYP1A1 is

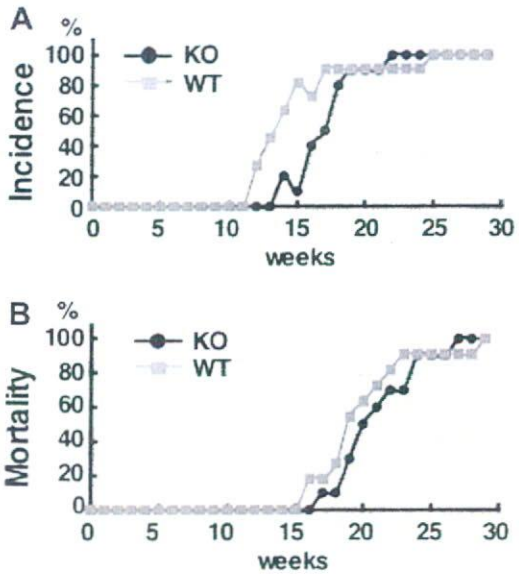

Fig. 4. B[*a*]P-induced tumor incidence and mortality of *AhRR(−/−)* mice. (A) WT (black; $n = 11$) and *AhRR*-KO (magenta; $n = 10$) mice were injected B[*a*]P subcutaneously twice. Tumor formation (A) and mortality (B) were observed as described in Materials and methods and shown as a percentage of the total.

known to be involved in both activation and detoxification of chemical carcinogens [16], "super-induction" of CYP1A1 in *AhRR(−/−)* mice is considered to shift the balance in favor of detoxification by accelerating the rate of drug metabolism to lower the carcinogenic intermediates of B[*a*]P.

Acknowledgments

We thank Yuko Kikuchi, Naomi Kaneko, Reiko Kawai, Mitsuru Okano and Masayoshi Noguchi for help during the experiments. We also thank Dr. Keisuke Yamashita and Ms. Yoko Nemoto for discussion and for clerical work, respectively. This work was supported in part by a grant from Solution Oriented Research for Science and Technology, Japan Science and Technology Agency and by a grant for Scientific Research from the Ministry of Health, Labor and Welfare of Japan.

References

[1] O. Hankinson, The aryl hydrocarbon receptor complex, Annu. Rev. Pharmacol. Toxicol. 35 (1995) 307–340.

[2] M.E. Hahn, The aryl hydrocarbon receptor: a comparative perspective, Comp. Biochem. Physiol. Part C Pharmacol. Toxicol. Endocrinol. 121 (1998) 23–53.

[3] J.P. Whitlock Jr., Induction of cytochrome P4501A1, Annu. Rev. Pharmacol. Toxicol. 39 (1999) 103–125.

[4] K. Kawajiri, Y. Fujii-Kuriyama, Cytochrome P450 gene regulation and physiological functions mediated by the aryl hydrocarbon receptor, Arch. Biochem. Biophys. 464 (2007) 207–212.

[5] R. Barouki, X. Coumoul, P.M. Fernandez-Salguero, The aryl hydrocarbon receptor, more than a xenobiotic-interacting protein, FEBS Lett. 581 (2007) 3608–3615.

[6] J. Mimura, M. Ema, K. Sogawa, Y. Fujii-Kuriyama, Identification of a novel mechanism of regulation of Ah (dioxin) receptor function, Genes Dev. 13 (1999) 20–25.

[7] T. Baba, J. Mimura, K. Gradin, A. Kuroiwa, T. Watanabe, Y. Matsuda, J. Inazawa, K. Sogawa, Y. Fujii-Kuriyama, Structure and expression of the Ah receptor repressor gene, J. Biol. Chem. 276 (2001) 33101–33110.

[8] T. Watanabe, I. Imoto, Y. Kosugi, Y. Fukuda, J. Mimura, Y. Fujii, K. Isaka, M. Takayama, A. Sato, J. Inazawa, Human arylhydrocarbon receptor repressor (AhRR) gene: genomic structure and analysis of polymorphism in endometriosis, J. Hum. Genet. 46 (2001) 342–346.

[9] H. Nishihashi, Y. Kanno, K. Tomuro, T. Nakahama, Y. Inouye, Primary structure and organ-specific expression of the rat aryl hydrocarbon receptor repressor gene, Biol. Pharm. Bull. 29 (2006) 640–647.

[10] S.I. Karchner, D.G. Franks, W.H. Powell, M.E. Hahn, Regulatory interactions among three members of the vertebrate aryl hydrocarbon receptor family: AHR repressor, AHR1, and AHR2, J. Biol. Chem. 277 (2002) 6949–6959.

[11] T. Hosoya, Y. Oda, S. Takahashi, M. Morita, S. Kawauchi, M. Ema, M. Yamamoto, Y. Fujii-Kuriyama, Defective development of secretory neurones in the hypothalamus of Arnt2-knockout mice, Genes Cells 6 (2001) 361–374.

[12] M. Ema, N. Ohe, M. Suzuki, J. Mimura, K. Sogawa, S. Ikawa, Y. Fujii-Kuriyama, Dioxin binding activities of polymorphic forms of mouse and human arylhydrocarbon receptors, J. Biol. Chem. 269 (1994) 27337–27343.

[13] E.C. Miller, J.A. Miller, Searches for ultimate chemical carcinogens and their reactions with cellular macromolecules, Cancer 47 (1981) 2327–2745.

[14] Y. Shimizu, Y. Nakatsuru, M. Ichinose, Y. Takahashi, H. Kume, J. Mimura, Y. Fujii-Kuriyama, T. Ishikawa, Benzo[a]pyrene carcinogenicity is lost in mice lacking the aryl hydrocarbon receptor, Proc. Natl. Acad. Sci. USA 97 (2000) 779–782.

[15] J. Mimura, K. Yamashita, K. Nakamura, M. Morita, T.N. Takagi, K. Nakao, M. Ema, K. Sogawa, M. Yasuda, M. Katsuki, Y. Fujii-Kuriyama, Loss of teratogenic response to 2,3,7,8-tetrachlorodibenzo-p-dioxin (TCDD) in mice lacking the Ah (dioxin) receptor, Genes Cells 2 (1997) 645–654.

[16] A. Conney, Induction of microsomal enzymes by foreign chemicals and carcinogenesis by polycyclic aromatic hydrocarbons: G.H.A. Clowes Memorial Lecture 42 (1982) 4875–4917.

[17] Q. Ma, Induction of CYP1A1. The AhR/DRE paradigm: transcription, receptor regulation, and expanding biological roles, Curr. Drug Metab. 2 (2001) 149–164.

Available online at www.sciencedirect.com
ScienceDirect
Biochemical and Biophysical Research Communications 364 (2007) 276–282
BBRC
www.elsevier.com/locate/ybbrc

Molecular mechanism of transcriptional repression of AhR repressor involving ANKRA2, HDAC4, and HDAC5

Motohiko Oshima [a,b], Junsei Mimura [a,b], Masayuki Yamamoto [a], Yoshiaki Fujii-Kuriyama [a,b,*]

[a] *Center for Tsukuba Advanced Research Alliance and Institute of Basic Medical Sciences, University of Tsukuba, 1-1-1 Tennoudai, Tsukuba 305-8577, Japan*
[b] *SORST, Japan Science and Technology Agency, 4-1-8 Honcho, Kawaguchi 332-0012, Japan*

Received 14 September 2007
Available online 11 October 2007

Abstract

The Aryl hydrocarbon receptor repressor (AhRR) has been proposed to inhibit Aryl hydrocarbon receptor (AhR) activity by competing with AhR for forming a heterodimer with AhR nuclear translocator (Arnt) and subsequently binding to the xenobiotic responsive elements (XRE). However, the precise mechanism of AhRR inhibitory activity remains unknown. Analysis of the inhibitory activity of AhRR on the expression of a TK promoter-driven reporter has localized a core repressor domain in the sequence of amino acid residue 555–701. The inhibitory activity of AhRR is sensitive to a histone deacetylase (HDAC) inhibitor, trichostatin A. By using the yeast two-hybrid screening method with the C-terminal sequence of AhRR as bait, we identified a binding partner, Ankyrin-repeat protein2 (ANKRA2), a protein known to interact with HDAC4 and HDAC5. RNA interference experiments using ANKRA2 and AhRR siRNAs indicate that ANKRA2 is important for transcriptional repression by AhRR. We have found that under normal conditions, *CYP1A1* gene is kept silent in MEF cells by AhRR/Arnt heterodimer, which binds to the XRE sequence in its promoter and recruits ANKRA2, HDAC4, and HDAC5 as co-repressors.

Keywords: Aryl hydrocarbon receptor (AhR); AhR repressor (AhRR); ANKRA2; HDAC4; HDAC5; CYP1A1; RFXANK

The Aryl hydrocarbon receptor (AhR) is a ligand-activated transcription factor that belongs to a superfamily with basic helix-loop-helix/Per-Arnt-Sim (bHLH-PAS) structural motifs and functions as an intracellular mediator of xenobiotic signaling pathways [1]. Normally, AhR exists within the cytoplasm in association with a complex of HSP90, XAP2, and p23. Upon binding a ligand such as tetrachlorodibenzo-*p*-dioxin (TCDD), the AhR complex translocates into the nucleus and forms a heterodimer with the structurally related AhR nuclear translocator (Arnt) [1]. Thereupon, the AhR/Arnt heterodimer binds to XRE (xenobiotic responsive elements) sequences in the promoter regions of the target genes encoding drug-metabolizing enzymes, such as *CYP1A1* and *CYP1B1* to enhance their expressions [2]. The AhR signaling pathway mediates not only the adaptive response required for the detoxification of xenobiotics, but also a variety of xenobiotics-induced toxicological effects such as tumor promotion, teratogenesis, and endocrine disruption [3–7]. In addition, AhR is also known to mediate multiple physiologic processes such as female reproduction [8,9].

During the course of our study on the AhR transcription factor, we found a novel bHLH-PAS family protein with a high similarity to AhR in the N-terminal bHLH-PAS A domain. In contrast, its C-terminal region shares a minimal degree of similarity to that of AhR and lacks the obvious PAS B domain of the ligand-binding site in AhR [10]. In transient DNA transfection assays, we found

* Corresponding author. Address: Center for Tsukuba Advanced Research Alliance and Institute of Basic Medical Sciences, University of Tsukuba, 1-1-1 Tennoudai, Tsukuba 305-8577, Japan. Fax: +81 29 853 7318.
E-mail address: ykfujii@tara.tsukuba.ac.jp (Y. Fujii-Kuriyama).

0006-291X/$ - see front matter © 2007 Elsevier Inc. All rights reserved.
doi:10.1016/j.bbrc.2007.09.131

that this novel protein inhibits AhR-dependent transactivation of the XRE-driven gene, and thus designated it AhR repressor (AhRR) [10].

Recently, AhRR orthologs have been reported in human [11,12], rat [11,13], and fish [14,15] and their genes have three conserved XRE sequences in the 5′-flanking promoter region. Accordingly, it has been reported that the AhRR expression is activated by the AhR/Arnt heterodimer in some cell lines [11,12] and multiple tissues of various species [10,12–14], indicating that AhRR participates in a negative feedback loop in the AhR signaling pathway [10,14,15].

Although the precise mechanism of inhibitory activity of AhRR remains to be elucidated, it has been proposed that AhRR competes with AhR for heterodimerization with Arnt and binding to the XRE sequence, a property that is likely to be mediated by N-terminal bHLH-PAS domains of these proteins [10].

In this study, we report that AhRR has a transcriptional repression domain within its C-terminal region, which exhibits a trichostatin A (TSA)-sensitive HDAC activity. By Cytotrap yeast two-hybrid screening with the C-terminal sequence of AhRR used as bait, we isolated Ankyrin-repeat protein2 (ANKRA2) as a binding partner to the AhRR C-terminal sequence.

Materials and methods

Plasmids. Fragments for AhRR(1–701 a.a.), AhRR(1–342 a.a.), AhRR(342–701 a.a.), AhRR(342–478 a.a.), AhRR(478–701 a.a.), AhRR(478–555 a.a.), AhRR(555–701 a.a.) were excised from pBOS-AhRR [10] and cloned into the pBOSGAL4DBD vector [16]. pG3TK-Luc was produced by inserting three copies of the GAL4 binding site excised from pG5EC and TK promoter sequence excised from pBSCAT2 into the XhoI site of pGL3 vector (Clontech). pBOSHA-AhRR was constructed as follows: pBOST7HA vector was constructed by inserting the blunt-ended BglII/PstI fragment of pGADT7 vector containing T7 promoter and HA epitope Tag into blunt-ended BamHI site of pEFBOS vector [17]. The EcoRI/SalI fragment excised from pBSKAhRR (Mimura, unpublished data) was inserted into the EcoRI and SalI site of pBOST7HA. pBOS-FLAG-ANKRA2 was constructed as follows: pBOST7FLAG vector was constructed by inserting the fragment containing the T7 promoter and FLAG epitope Tag cleaved from pGADT7FLAG vector into blunt-ended BamHI site of pEFBOS vector. Mouse ANKRA2 cDNA was amplified with a pair of primers, 5′-CatcgatACATGGCTACATCTGCAAAT-3′ and 5′-CggatccTCACTCCCTGATGTTCTGAA-3′ as the 5′ and 3′ primers, respectively. The amplified cDNA fragment was digested with ClaI and BamHI, and inserted into the ClaI and BamHI site of pBOST7FLAG. Expression plasmids encoding HDAC4-FLAG and HDAC5-FLAG were kindly provided by Dr. Stuart L. Schreiber (Harvard University, MA, USA).

Antibody production. Recombinant glutathione S-transferase (GST)-tagged mouse AhRR (342–701 a.a.) and recombinant maltose-binding protein (MBP)-tagged mouse AhRR (342–701 a.a.) were expressed in *Escherichia coli* and purified with Glutathione Sepharose 4B (Amersham Biosciences) and amylose resin (New England Biolabs), respectively, according to the manufacturer's protocols. Polyclonal rabbit antisera were raised against the recombinant GST-AhRR (342–701 a.a.) and further affinity-purified with the recombinant MBP-AhRR (342–701 a.a.) (Hokudo Inc., Japan).

Cell culture. Mouse embryonic fibroblast (MEF) cells were isolated from C57B/6J mice. COS-7, MEF, and Hepa-1c1c7 (Hepa-1) cells were maintained in high glucose Dulbecco's modified Eagle's medium (Sigma) supplemented with 10% fetal bovine serum (Sigma) and penicillin/streptomycin (Invitrogen) under 5.0% CO_2 at 37 °C.

Luciferase assay. Hepa-1 cells (5.0×10^4 cells/well) were grown in 24-well dishes for 24 h and were transfected with the expression plasmids indicated in the figure legends, pG3TK-Luc and the expression plasmids for sea pansy luciferase as an internal control using Lipofectamine™ (Invitrogen). Forty-eight hours after transfection, the cells were harvested and luciferase was quantified by using the dual-luciferase reporter assay system (Promega) according to the manufacturer's protocols. For control of transfection efficiency, firefly luciferase activity was normalized to cotransfected sea pansy luciferase activity as a standard.

Coimmunoprecipitation and immunoblot analysis. Cell lysates from the transfected COS-7 and MEF cells were prepared as described and used for immunoblot analysis either directly or after immunoprecipitation. Immunoprecipitation with anti-Flag M2 agarose (Sigma) or anti-HA agarose (Sigma) was performed for 12 h and the immunoprecipitates were washed according to the published procedure for immunoblot analysis. Immunoblot analysis was performed as described [7] using anti-FLAG (Sigma), anti-HA (Sigma), anti-Tubulin (Sigma), and anti AhRR antibodies.

RNA interference experiments. The siRNAs for mouse ANKRA2 or mouse AhRR were designed and synthesized by B-Bridge International Inc. The coding sequences were: ANKRA2, (5′-AGGAAAAGGUCGAG AAAGUdTdT-3′) and AhRR, (5′-GGAAAGGCCUUGUGGCUAAdT dT-3′). Hepa-1 cells or MEF cells (5.0×10^4 cells/well) were transfected with siRNA for ANKRA2 (20 pmol) or AhRR (50 pmol) with or without expression plasmids by using Lipofectamine 2000 (Invitrogen) according to the manufacturer's instructions.

Quantification of mRNA. Total RNAs are extracted from cells using Isogen (Nippon Gene, Tokyo) and reverse transcribed by Superscript II (Invitrogen). Real-time PCR was carried out in ABI PRISM 7700 sequence detection system using the following primer sets: ANKRA2, forward (5′-TCTACCACACCTCTGTTAGC-3′) and reverse (5′-GCA CTTTCTCGACCTTTTCC-3′); AhRR, forward (5′-GCTTTCTGTCCT GCGCCTC-3′) and reverse (5′-TCCTTCCTGCACGGGGAAC-3′); CY P1A1, forward (5′-GGACATTTGAGAAGGGCCAC-3′) and reverse (5′-CGTCCAGCTTCCTGTCCTGA-3′); actin, forward (5′-GACAGGAT GCAGAAGGAGAT-3′) and reverse (5′-TTGCTGATCCACATCTGC TG-3′).

Cytotrap yeast two-hybrid assay. The CytoTrap™ (Stratagene) yeast screening was performed with a murine thymus cDNA library (Stratagene) and pSos-AhRR (342–701) as prey and bait, respectively, according to the manufacturer's instructions.

Results

Functional characterization of the AhRR transcriptional repression domain

We previously reported that AhRR inhibits the transcription activity of Arnt [10]. In order to confirm transcriptional repression activity and to localize the transcriptional repression domain of AhRR, we fused a series of AhRR deletion mutants to the GAL4 DNA binding domain (GAL) (Fig. 1A). These fragments were transfected into Hepa-1 cells, along with a luciferase reporter gene driven by three GAL4 binding sites and the TK promoter (Fig. 1A). The luciferase activity driven by the TK promoter was repressed 5.2-fold by the transfection with plasmid, GAL4DBD-AhRR (1–701) (Fig. 1B). Plasmids encoding the fusion proteins, GAL4DBD-AhRR (342–701), (478–701), and (555–701) also repressed luciferase expression 5.6-, 4.9- and 3.7-fold, respectively, while plasmids of AhRR (1–342), AhRR (342–478), and AhRR

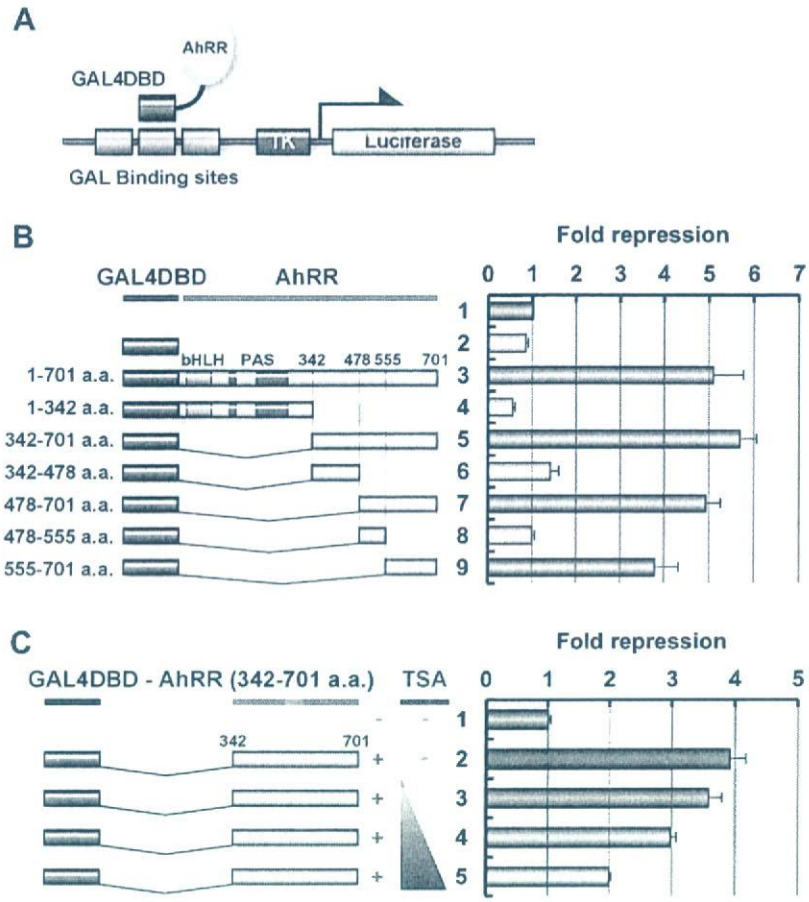

Fig. 1. The carboxy-terminal half of AhRR shows a repressor activity, which is sensitive to the HDAC inhibitor, TSA. (A) Schematic representation of luciferase reporter assay. (B) Transcriptional repression activity of AhRR. Hepa-1 cells were transiently transfected with the expression plasmids of GAL4DBD-AhRR and GAL-TK-Luc reporter gene containing three GAL binding sites. Cell extracts were prepared 48 h after transfection and used for luciferase assays. The fold repression is relative to the reporter gene alone. (C) Effects of TSA on AhRR-mediated transcriptional repression. The transfections were performed as described in (B), Cells were treated with increasing amounts (2, 4, and 8 ng/ml) of TSA 24 h after transfection and then, 12 h later, whole cell extracts were prepared and used for luciferase assays.

(478–555) did not significantly repress luciferase expression. These data localized a core region needed for transcriptional repression by AhRR to the sequence of amino acid 555–701.

To investigate how the repression activity of the AhRR fragment (342–701) functions in the TK promoter-driven reporter system, we used the HDAC inhibitor, TSA, which reversed the repression of reporter gene expression by the AhRR fragment (342–701) in a dose-dependent manner (Fig. 1C). These results suggest that the repression activity of the AhRR C-terminus is due to an HDAC activity. Since the C-terminal sequence of AhRR is well conserved among multiple mammalian species (Supplementary Fig. S1), we next searched for transcriptional corepressor, which interact with the AhRR C-terminus.

Isolation of ANKRA2 as a factor interacting with AhRR and interaction of AhRR with ANKRA2 and HDAC4 or HDAC5

To isolate a corepressor of AhRR, we performed a Cytotrap yeast two-hybrid screen with the C-terminal fragment of AhRR (342–701) used as bait (Fig. 2A) and isolated several clones including Dhx8, EB1, EB3, p21, Prostaglandin E receptor, EGF-containing fibrin-like extracellular matrix protein1, and ANKRA2. We chose ANKRA2 for further work in this paper, because ANKRA2 is reported to interact with HDAC4 and HDAC5 [18]. Recently, its mammalian paralogue, RFXANK has also been reported to interact with HDAC4 and HDAC5 [18] and to repress MHC class II promoter activation through association with HDAC4 and HDAC5 [19]. Taken together, these results suggest a potential role of ANKRA2 as mediator in transcriptional repression. ANKRA2 is a protein of 312 amino acids with consecutive 3 ankyrin repeats and the cDNA encoded a C-terminal fragment, amino acid 117–312 (Fig. 2A).

To address whether a physical interaction occurs between AhRR and ANKRA2, whole cell extracts from COS-7 cells cotransfected with expression plasmids for HA-tagged AhRR and FLAG-tagged ANKRA2 were used for *in vivo* coimmunoprecipitation studies. As expected, when the cell extracts were immunoprecipitated with an anti-FLAG antibody, AhRR was coimmunoprecipitated

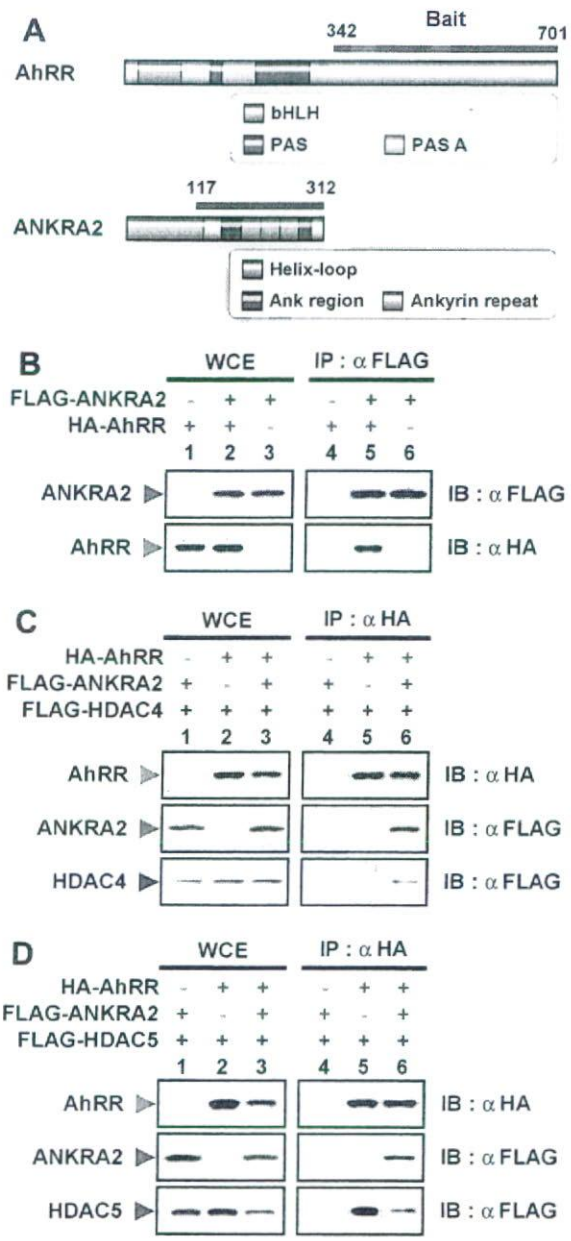

Fig. 2. Physical interaction of AhRR with ANKRA2 and HDAC4 or HDAC5. (A) Schematic diagrams of AhRR and ANKRA2. The carboxy-terminal half of AhRR was used as bait in a yeast two-hybrid screen. The AhRR bait interacted with a fragment (117–312 amino acid) of ANKRA2. ANKRA2 is a protein of 312 amino acids that contains an amino-terminal helix-loop-helix domain and four ankyrin repeats at the C terminus. (B) COS-7 cells were cotransfected with expression plasmids of HA-tagged AhRR and FLAG-tagged ANKRA2. Whole cell extracts were prepared 48 h after transfection and immunoprecipitated (IP) with anti-FLAG antibodies. Immunoprecipitates were analyzed by immunoblot with the indicated antibodies. Crude lysates were analyzed by immunoblot to control protein expressions (WCE). (C) COS-7 cells were cotransfected with expression plasmids of HA-tagged AhRR, FLAG-tagged ANKRA2 and either FLAG-tagged HDAC4 or HDAC5. Cell extracts were prepared 48 h after transfection and immunoprecipitated (IP) with anti-HA antibodies. Proteins were analyzed by immunoblot as described above.

with ANKRA2 (Fig. 2B, lane 5). We next asked if HDAC4 and HDAC5 also interact with AhRR. Whole cell extracts from COS-7 cells cotransfected with expression plasmids for HA-tagged AhRR and FLAG-tagged ANKRA2 together with either FLAG-tagged HDAC4 or FLAG-tagged HDAC5 were immunoprecipitated with an anti-HA antibody. HDAC4 was coimmunoprecipitated with AhRR only when ANKRA2 was cotransfected (Fig. 2C, lane 6). On the other hand, HDAC5 was also coimmunoprecipitated with AhRR even in the absence of ANKRA2, indicating that HDAC5 interacts with AhRR either directly or through ANKRA2 (Fig. 2D, lanes 5 and 6).

Depletion of ANKRA2 by siRNA attenuates transcriptional repression activity of AhRR

If ANKRA2 is a corepressor for AhRR, downregulation of the endogenous level of ANKRA2 by siRNA against ANKRA2 should reverse the transcriptional repression activity of AhRR. To confirm the requirement of ANKRA2 for the repression activity of AhRR, Hepa-1 cells were transiently transfected with expression plasmids for GAL-AhRR together with ANKRA2 siRNA or control siRNA. As shown in Fig. 3A, ANKRA2 siRNA transfection significantly reduced the expression of ANKRA2 mRNA. As expected, when the cells were treated with ANKRA2 siRNA, the repression activity of AhRR was significantly reversed as compared with that observed in cells treated with control siRNA (Fig. 3B).

To further investigate whether ANKRA2 is required for the endogenous AhRR/Arnt heterodimer to repress the XRE-driven transcription of endogenous target genes such as *CYP1A1*, we conducted RNA interference experiments in MEF cells. When MEF cells were transfected with ANKRA2 siRNA, endogenous ANKRA2 mRNA levels were significantly lowered both in the presence or absence of an AhR ligand, 3MC (Fig. 3C). Under normal conditions, CYP1A1 mRNA expression was barely detectable, but knockdown of ANKRA2 by ANKRA2 siRNA caused a small, but significant increase in basal CYP1A1 mRNA levels (Fig. 3D, lane 1). When treated with 3MC for 6 h, MEF cells inducibly expressed CYP1A1 mRNA to a similar level in the presence and absence of ANKRA2 siRNA (Fig. 3D, lane 2). These results suggest that in the silent state of MEF cells, the AhRR-ANKRA2 suppressor complex is involved in silencing the CYP1A1 basal expression, while under inducing conditions, ANKRA2 does not greatly affect the inducible expression of *CYP1A1* gene.

To confirm that the AhRR–ANKRA2 repressor complex silences the transcription of endogenous CYP1A1 in MEF cells, we used siRNA against AhRR. As previously reported in many other cell lines and tissues, AhRR mRNA and protein was constitutively expressed in MEF cells under normal conditions and was further enhanced in response to 3MC (Fig. 3E, lanes 1 and 2, and F). When MEF cells were transfected with AhRR siRNA, both mRNA and protein levels of AhRR were markedly downregulated (Fig. 3E, lanes 1 and 3, and F). In agreement with the result of the ANKRA2 siRNA experiment, treatment of AhRR siRNA increased CYP1A1 mRNA under normal

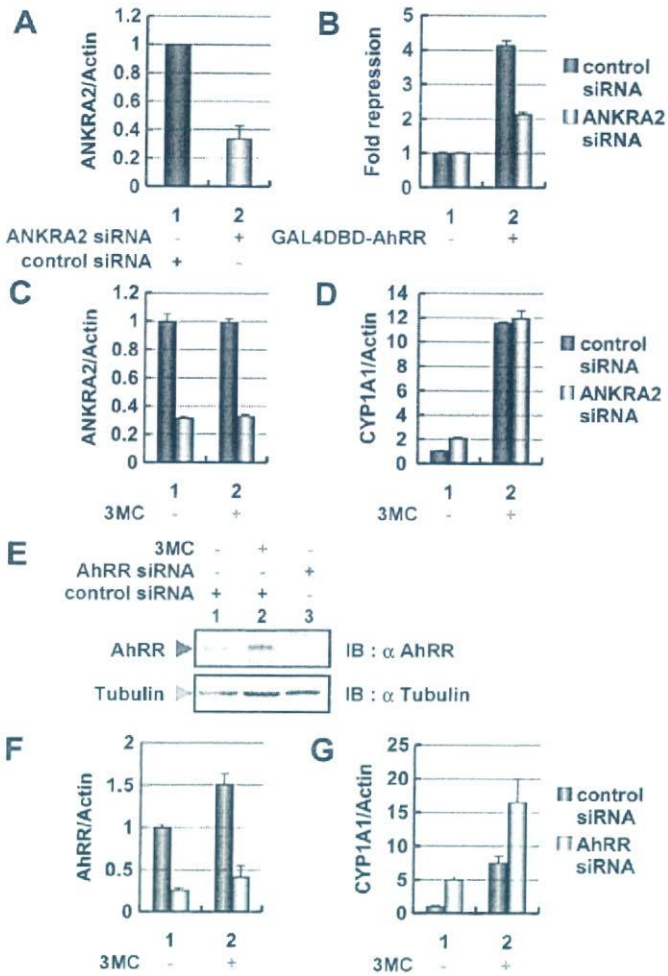

Fig. 3. Effects of ANKRA2 and AhRR siRNAs on the transcriptional repression activity of AhRR. (A) Hepa-1 cells were transiently transfected with ANKRA2 or control siRNA and 48 h after transfection, RNA were prepared from the transfected cells. ANKRA2 mRNA was quantified by RT-PCR method. (B) Hepa-1 cells were transiently transfected with GAL4DBD-AhRR and a reporter gene of GAL-TK-Luc, along with ANKRA2 siRNA or control siRNA. Cell extracts were prepared 48 h after transfection and used for luciferase assays. (C–G) MEF cells were transiently transfected with ANKRA2 siRNA (C and D) or AhRR siRNA (E–G) or control siRNA. After 48 h of transfection, cells were treated with 2 μM of 3MC or Me_2SO and then, 24 h later, cell extracts were prepared and indicated mRNA expression level was quantified using real time RT-PCR (C, D, E, and F) or immunoblot analysis (E).

conditions to even a higher extent than ANKRA2 siRNA treatment (Fig. 3G, lane 1). Interestingly, AhRR siRNA also further increased the induced expression of CYP1A1 mRNA in response to 3MC, as compared with the expression in cells treated with control siRNA, suggesting the existence of an ANKRA2-independent repression mechanism by AhRR (Fig. 3G, lane 2). As reported previously, AhRR may prevent AhR from forming a heterodimer with Arnt in a competitive manner, thereby blocking the binding of AhR to the XRE sequence in the absence of ANKRA2. Taken together, these results indicate that in a silent state of CYP1A1 expression under normal conditions, AhRR represses the expression of *CYP1A1* gene by binding the XRE sequence and recruiting ANKRA2, HDAC4 and/or HDAC5.

Discussion

We previously reported that AhRR repressed AhR transcription activity by competing with Arnt in AhR/Arnt heterodimerization, as well as by binding the XRE sequence in the promoter of CYP1A1 gene. Since Arnt has a weak transcription activity at its C-terminal end, it is possible that AhRR could have some inhibitory activity to compensate for Arnt transcription activity. In this report, we first demonstrated that the C-terminus (555–701 a.a.) of AhRR shows a transcription inhibitory activity which was sensitive to the HDAC inhibitor, TSA, suggesting that AhRR which binds the XRE sequence recruits a HDAC protein. To isolate factors that interact with the C-terminal sequence of AhRR, we utilized the Cytotrap yeast two-hybrid screening method using the C-terminal sequence of AhRR as bait, resulting in isolation of a fragment (113–312 a.a.) of ANKRA2 consisting of 312 amino acids and containing three ankyrin (ANK) repeats. The isolated ANKRA2 fragment was shown to physically interact with AhRR (Fig. 2B). ANK repeats are one of the most common protein sequence motifs mediating protein–protein interactions, but they have not been clarified to bind any specific amino acid sequence or structure. Rather, they are thought to bind a variety of proteins through adaptive alterations in their binding surface features and in the domain size of the ANK repeat by sequence duplication or deletion [20]. Recent studies have demonstrated that ANKRA2 also interacts with megalin [21] and the α-subunit of rat large-conductance Ca^{2+}-activated K^+ channel (rSlo) [22]. According to Rader et al. [21], the C-terminus (177–312 a.a.) of ANKRA2 interacts with a proline-rich motif (PXXPXXP) within the 19 amino acid sequence of the magalin tail, and Lim and Park [22] have shown that 52–150 a.a. of ANKRA2 interacts with the C-terminal end (1119–1210 a.a.) of rSlo Channel. Since there is no apparent sequence similarity in the ANKRA2-interacting domains of megalin, rSlo and AhRR, the precise molecular mechanisms how ANKRA2 interacts with these proteins remain to be investigated.

Our coimmunoprecpitation experiments have revealed that HDAC4 interacts with AhRR in an ANKRA2-dependent manner. HDAC5 may interact with AhRR either directly or via ANKRA2, when the previous report is taken into account [18]. It remains to be studied how HDAC4 and HDAC5 are recruited on the surface of the AhRR and ANKA2 complex, reciprocally or simultaneously. ANKRA2 is also abundantly and ubiquitously expressed in various tissues of mice [21] and cultured cells such as Hepa-1, HeLa and MEF cells used in this study (data not shown). For functional analysis of ANKRA2 and AhRR, we used siRNA to knock down gene expres-

sion. In Hepa-1 cells, repression of TK promoter-driven luciferase activity by GAL4DBD-AhRR was reversed by the addition of ANKRA2 siRNA, indicating that the repression activity of AhRR required ANKRA2. Treatment of MEF cells with ANKRA2 siRNA significantly activated the expression of *CYP1A1* under normal conditions. In contrast, the siRNA treatment had apparently no effect on the enhanced CYP1A1 expression in response to the inducer. These results suggest that under normal conditions, a silent state of *CYP1A1* gene expression is not merely due to the lack of a transcription activator, but resulted from negative regulation by a heterodimer of AhRR and Arnt, which recruits ANKRA2. This observation was substantiated by the experiments using AhRR siRNA, which significantly enhanced the expression of *CYP1A1* gene under normal conditions to even a higher level than did ANKRA2 siRNA under the non-inducing conditions. The greater effect of AhRR siRNA on CYP1A1 expression becomes more pronounced under inducing conditions. These observations could be explained by a two step inhibitory mechanism. First, AhRR inhibits the transcription activity of AhR in an ANKRA2-independent manner, by competing with AhR for forming a heterodimer with Arnt and binding the XRE sequence, as reported previously. Next, AhRR bound to the XRE sequence recruits ANKRA2 and HDAC4 and/or HDAC5 for more efficient repression. In the presence of the inducer 3MC, AhRR synthesis is accelerated so that the AhRR siRNA treatment displays a greater effect on the inducible expression of CYP1A1 than ANKRA2 siRNA. Recently, we have found that the silent state of CYP1A1 is actually negatively regulated by the AhRR system in macrophages (unpublished data). We will be investigating how this silencing mechanism involving AhRR and ANKRA2 functions in different cell types and how it affects target genes other than *CYP1A1* under normal conditions.

Acknowledgments

We thank Mrs. Y. Nemoto for clerical work. This work was funded in part by Solution Oriented Research for Science and Technology, Japan Science and Technology Agency and by a Grant for Scientific Research from the Ministry of Health, Labor, and Welfare of Japan.

Appendix A. Supplementary data

Supplementary data associated with this article can be found, in the online version, at doi:10.1016/j.bbrc.2007.09.131.

References

[1] J. Mimura, Y. Fujii-Kuriyama, Functional role of AhR in the expression of toxic effects by TCDD, Biochim. Biophys. Acta 1619 (2003) 263–268.

[2] A. Fujisawa-Sehara, K. Sogawa, M. Yamane, Y. Fujii-Kuriyama, Characterization of xenobiotic responsive elements upstream from the drug-metabolizing cytochrome P-450c gene: A similarity to glucocorticoid regulatory elements, Nucleic Acids Res. 15 (1987) 4179–4191.

[3] N.M. Brown, P.A. Manzolillo, J.X. Zhang, J. Wang, C.A. Lamartiniere, Prenatal TCDD and predisposition to mammary cancer in the rat, Carcinogenesis 19 (1998) 1623–1629.

[4] A. Gibbons, Dioxin tied to endometriosis, Science 262 (1993) 1373.

[5] J. Mimura, K. Yamashita, K. Nakamura, M. Morita, T.N. Takagi, K. Nakao, M. Ema, K. Sogawa, M. Yasuda, M. Katsuki, Y. Fujii-Kuriyama, Loss of teratogenic response to 2,3,7,8-tetrachlorodibenzo-p-dioxin (TCDD) in mice lacking the ah (dioxin) receptor, Genes Cells 2 (1997) 645–654.

[6] Y. Shimizu, Y. Nakatsuru, M. Ichinose, Y. Takahashi, H. Kume, J. Mimura, Y. Fujii-Kuriyama, T. Ishikawa, Benzo[a]pyrene carcinogenicity is lost in mice lacking the aryl hydrocarbon receptor, Proc. Natl. Acad. Sci. USA 97 (2000) 779–782.

[7] F. Ohtake, K. Takeyama, T. Matsumoto, H. Kitagawa, Y. Yamamoto, K. Nohara, C. Tohyama, A. Krust, J. Mimura, P. Chambon, J. Yanagisawa, Y. Fujii-Kuriyama, S. Kato, Modulation of oestrogen receptor signalling by association with the activated dioxin receptor, Nature 423 (2003) 545–550.

[8] T. Baba, J. Mimura, N. Nakamura, N. Harada, M. Yamamoto, K. Morohashi, Y. Fujii-Kuriyama, Intrinsic function of the aryl hydrocarbon (dioxin) receptor as a key factor in female reproduction, Mol. Cell. Biol. 25 (2005) 10040–10051.

[9] B.D. Abbott, J.E. Schmid, J.A. Pitt, A.R. Buckalew, C.R. Wood, G.A. Held, J.J. Diliberto, Adverse reproductive outcomes in the transgenic ah receptor-deficient mouse, Toxicol. Appl. Pharmacol. 155 (1999) 62–70.

[10] J. Mimura, M. Ema, K. Sogawa, Y. Fujii-Kuriyama, Identification of a novel mechanism of regulation of ah (dioxin) receptor function, Genes Dev. 13 (1999) 20–25.

[11] T. Baba, J. Mimura, K. Gradin, A. Kuroiwa, T. Watanabe, Y. Matsuda, J. Inazawa, K. Sogawa, Y. Fujii-Kuriyama, Structure and expression of the ah receptor repressor gene, J. Biol. Chem. 276 (2001) 33101–33110.

[12] Y. Tsuchiya, M. Nakajima, S. Itoh, M. Iwanari, T. Yokoi, Expression of aryl hydrocarbon receptor repressor in normal human tissues and inducibility by polycyclic aromatic hydrocarbons in human tumor-derived cell lines, Toxicol. Sci. 72 (2003) 253–259.

[13] M. Korkalainen, J. Tuomisto, R. Pohjanvirta, Primary structure and inducibility by 2,3,7,8-tetrachlorodibenzo-p-dioxin (TCDD) of aryl hydrocarbon receptor repressor in a TCDD-sensitive and a TCDD-resistant rat strain, Biochem. Biophys. Res. Commun. 315 (2004) 123–131.

[14] S.I. Karchner, D.G. Franks, W.H. Powell, M.E. Hahn, Regulatory interactions among three members of the vertebrate aryl hydrocarbon receptor family: AHR repressor, AHR1, and AHR2, J. Biol. Chem. 277 (2002) 6949–6959.

[15] B.R. Evans, S.I. Karchner, D.G. Franks, M.E. Hahn, Duplicate aryl hydrocarbon receptor repressor genes (ahrr1 and ahrr2) in the zebrafish danio rerio: Structure, function, evolution, and AHR-dependent regulation in vivo, Arch. Biochem. Biophys. 441 (2005) 151–167.

[16] M. Ema, M. Suzuki, M. Morita, K. Hirose, K. Sogawa, Y. Matsuda, O. Gotoh, Y. Saijoh, H. Fujii, H. Hamada, Y. Fujii-Kuriyama, cDNA cloning of a murine homologue of drosophila single-minded, its mRNA expression in mouse development, and chromosome localization, Biochem. Biophys. Res. Commun. 218 (1996) 588–594.

[17] S. Mizushima, S. Nagata, pEF-BOS, a powerful mammalian expression vector, Nucleic Acids Res. 18 (1990) 5322.

[18] A.H. Wang, S. Gregoire, E. Zika, L. Xiao, C.S. Li, H. Li, K.L. Wright, J.P. Ting, X.J. Yang, Identification of the ankyrin repeat proteins ANKRA and RFXANK as novel partners of class IIa histone deacetylases, J. Biol. Chem. 280 (2005) 29117–29127.

[19] T.A. McKinsey, K. Kuwahara, S. Bezprozvannaya, E.N. Olson, Class II histone deacetylases confer signal responsiveness to the ankyrin-repeat proteins ANKRA2 and RFXANK, Mol. Biol. Cell 17 (2006) 438–447.

[20] S.G. Sedgwick, S.J. Smerdon, The ankyrin repeat: A diversity of interactions on a common structural framework, Trends Biochem. Sci. 24 (1999) 311–316.

[21] K. Rader, R.A. Orlando, X. Lou, M.G. Farquhar, Characterization of ANKRA, a novel ankyrin repeat protein that interacts with the cytoplasmic domain of megalin, J. Am. Soc. Nephrol. 11 (2000) 2167–2178.

[22] H.H. Lim, C.S. Park, Identification and functional characterization of ankyrin-repeat family protein ANKRA as a protein interacting with BKCa channel, Mol. Biol. Cell 16 (2005) 1013–1025.

Arteriosclerosis, Thrombosis, and Vascular Biology

JOURNAL OF THE AMERICAN HEART ASSOCIATION

American Heart Association®

Learn and Live℠

A Novel Class of Prolyl Hydroxylase Inhibitors Induces Angiogenesis and Exerts Organ Protection Against Ischemia

Masaomi Nangaku, Yuko Izuhara, Shunya Takizawa, Toshiharu Yamashita, Yoshiaki Fujii-Kuriyama, Osamu Ohneda, Masayuki Yamamoto, Charles van Ypersele de Strihou, Noriaki Hirayama and Toshio Miyata

Arterioscler. Thromb. Vasc. Biol. 2007;27;2548-2554; originally published online Oct 11, 2007;

DOI: 10.1161/ATVBAHA.107.148551

Arteriosclerosis, Thrombosis, and Vascular Biology is published by the American Heart Association. 7272 Greenville Avenue, Dallas, TX 72514

 Print ISSN: 1079-5642. Online ISSN: 1524-4636

A Novel Class of Prolyl Hydroxylase Inhibitors Induces Angiogenesis and Exerts Organ Protection Against Ischemia

Masaomi Nangaku, Yuko Izuhara, Shunya Takizawa, Toshiharu Yamashita, Yoshiaki Fujii-Kuriyama, Osamu Ohneda, Masayuki Yamamoto, Charles van Ypersele de Strihou, Noriaki Hirayama, Toshio Miyata

Objective—Hypoxia inducible factor (HIF) plays a pivotal role in the adaptation to ischemic conditions. Its activity is modulated by an oxygen-dependent hydroxylation of proline residues by prolyl hydroxylases (PHD).

Methods and Results—We discovered 2 unique compounds (TM6008 and TM6089), which inhibited PHD and stabilized HIF activity in vitro. Our docking simulation studies based on the 3-dimensional structure of human PHD2 disclosed that they preferentially bind to the active site of PHD. Whereas PHD inhibitors previously reported inhibit PHD activity via iron chelation, TM6089 does not share an iron chelating motif and is devoid of iron chelating activity. In vitro Matrigel assays and in vivo sponge assays demonstrated enhancement of angiogenesis by local administration of TM6008 and TM6089. Their oral administration stimulated HIF activity in various organs of transgenic rats expressing a hypoxia-responsive reporter vector. No acute toxicity was observed up to 2 weeks after a single oral dose of 2000 mg/kg for TM6008. Oral administration of TM6008 protected neurons in a model of cerebrovascular disease. The protection was associated with amelioration of apoptosis but independent of enhanced angiogenesis.

Conclusions—The present study uncovered beneficial effects of novel PHD inhibitors preferentially binding to the active site of PHD. (***Arterioscler Thromb Vasc Biol.* 2007;27:2548-2554.**)

Key Words: hypoxia ■ hypoxia inducible factor ■ structure based drug design ■ stroke ■ ischemia

Oxygen supply declines under ischemic conditions in many human vascular diseases including ischemic heart disease, chronic kidney failure, and stroke. The resulting hypoxia causes functional impairment of cells as well as structural tissue damage and triggers a broad spectrum of cellular defenses such as angiogenesis, erythropoiesis, glycolysis, and antioxidative enzymes.

Hypoxia-inducible factor (HIF), a heterodimeric nuclear factor, is a crucial intermediate in these defensive mechanisms.[1–3] Under normoxic conditions, HIF is constitutively transcribed and translated. Its stability is drastically reduced by the oxygen-dependent enzymatic hydroxylation of proline residues by prolyl hydroxylases (PHD).[4–9] Hydroxylated HIF recruits the E3-ubiquitin ligase, von Hippel Lindau protein (pVHL)[10,11] which, in turn, tags HIF with ubiquitin groups and targets it for degradation by the proteasome.[12,13] Under hypoxic conditions, HIF is not hydroxylated but binds to its heterodimeric partner HIF-1β. The resulting protein complex transactivates in the nucleus a host of genes involved in the adaptation to hypoxic stress.[14]

Activation of HIF may prove therapeutic for vascular disorders. Most treatments for ischemic and hypoxic disorders are currently focused on symptomatic relief and correction of etiologic factors. Drugs dissolving thrombi are also used to restore blood flow in the acute phase. As yet no compound enhancing organ resistance to hypoxia is clinically available. HIF activates a "master gene" switch that results in a broad and coordinated downstream reaction, protecting tissues against the consequences of hypoxia. The availability of less cumbersome non-toxic small molecular activators of HIF should prove very useful for therapeutic intervention.[15,16]

To obtain such novel compounds and to understand a molecular mechanism of PHD inhibition, we performed docking simulation based on the 3-dimensional structure of human PHD2. We further documented the in vitro and in vivo effectiveness of the novel PHD inhibitors we identified.

Materials and Methods

Please see the supplemental data section at http://atvb.ahajournals.org for detailed Methods.

Original received May 24, 2007; final version accepted September 26, 2007.

From the Division of Nephrology and Endocrinology (M.N.), University of Tokyo School of Medicine, Japan; the Institute of Medical Sciences (Y.I., S.T., T.M.), Divisions of Nephrology, Hypertension, and Metabolism and of Neurology, Tokai University School of Medicine, Kanagawa, Japan; the Center for Tsukuba Advanced Research Alliance and Institute of Basic Medical Sciences (T.Y., O.O.), University of Tsukuba, Japan; the Center for Tsukuba Advanced Research Alliance (Y.F.-K.), University of Tsukuba, Japan; the Center for Tsukuba Advanced Research Alliance and JST-ERATO Environmental Response Project (M.Y.), University of Tsukuba, and the Department of Medical Biochemistry, Tohoku University Graduate School of Medicine, Sendai, Japan; the Service de Nephrologie (C.v.Y.d.S.), Universite Catholique de Louvain, Brussels, Belgium; and the Basic Medical Science and Molecular Medicine (N.H.), Tokai University School of Medicine, Kanagawa, Japan.

Correspondence to Toshio Miyata, MD, PhD, Institute of Medical Sciences and Division of Nephrology, Hypertension and Metabolism, Tokai University School of Medicine, Isehara, Kanagawa 259-1193, Japan. E-mail t-miyata@is.icc.u-tokai.ac.jp

Arterioscler Thromb Vasc Biol **is available at http://atvb.ahajournals.org** **DOI: 10.1161/ATVBAHA.107.148551**

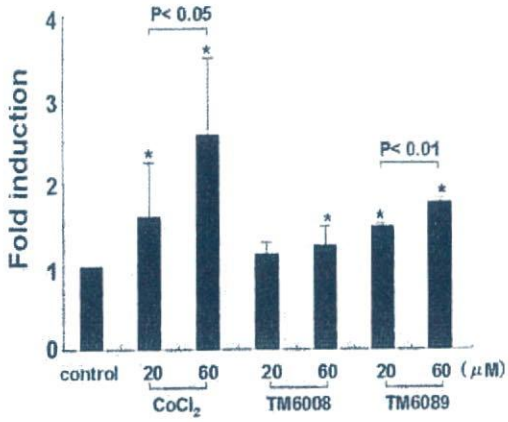

Figure 1. Stimulation of HIF-dependent luciferase reporter gene expression. IRPTC expressing the 7xHRE/Luc plasmid were incubated with the tested compounds. Cobalt chloride was used as a positive control. Results from 3 independent experiments are averaged and shown as fold increase above unstimulated control cells. *$P<0.05$ vs control.

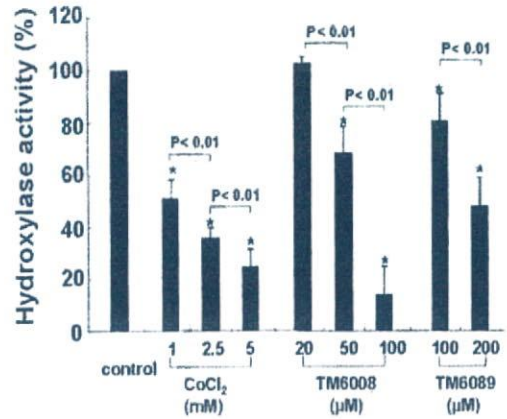

Figure 2. Inhibition of PHD activity. Results from 3 independent experiments are averaged and shown as the percentage of inhibition of ODD-dependent hydroxylase activity. *$P<0.01$ vs control.

Docking Simulations

The X-ray crystal structure of human PHD2 was obtained from the Protein Data Bank[17] (PDB code: 2HBT). Throughout the present study, the software system MOE (Molecular Operating Environment, version 2005.06) and the MMFF94s force field[18] were used. Binding sites were characterized using the alpha site finder function[19] in MOE. The docking of small molecules and the target sites was performed by the program Ph4Dock.[20]

PHD Activity

PHD activity was determined as described by Kaule et al.[21] In brief, mitochondrial fraction of IRPTC homogenates was reacted with the tested compounds and ODD peptide of HIF-1α. ODD-dependent hydroxylase activity was assessed by counting the radioactivity of [1-^{14}C]-succinate converted from [5-^{14}C]-2-OG by PHD.

Transition Metal Chelation

The chelating activity of the tested compounds for transition metal ions was measured by the method of Price et al[22] with some modifications.

Capillary Network Formation

Capillary network formation was examined by Matrigel assays (BD Biosciences) as described previously.[23]

Sponge Assays

Sponge angiogenesis assays were performed as described previously.[24]

Hypoxia-Sensing Transgenic Rat

Stimulation of the HIF-HRE system by systemic administration of TM6008 or TM6089 was evaluated using the hypoxia-sensing transgenic rat strain.[24] Expression of the hypoxia-responsive luciferase gene was estimated by semiquantitative RT-PCR as described previously.[25]

Cerebral Ischemic Injury Model

Transient global ischemia of Mongolian gerbils was achieved by bilateral carotid occlusion.[26] Animals were then randomly divided into 3 experimental groups: Groups 1 (TM6008) and 2 (vehicle) animals underwent transient global ischemia. Group 3 animals were sham-operated and served as controls.

We also measured cortical microperfusion by laser-Doppler flowmetry in gerbil forebrain ischemia treated with TM6008 or vehicle.

Statistics

Differences among groups were assessed by Kruskal-Wallis test or ANOVA. The statistical significance was determined by 2-tailed Mann–Whitney U test or Student t test. Data are expressed as means±SD. Values are considered significant at $P<0.05$.

Results

Identification of Novel HIF-Stimulating Compounds

Thirty-seven compounds that have structural similarities to FG-0041, a previously reported PHD inhibitor supposedly acting through iron chelation,[27] were selected from a chemical database. The chemical structures of these compounds are shown in supplemental Figure I. Their HIF-stimulating activity was tested by an in vitro screening assay which used cells expressing luciferase controlled by hypoxia responsive element (HRE) (supplemental Figure II). Cobalt, a well known chemical mimicker of hypoxia by stabilizing HIF-α subunit,[28] was used as a positive control. Two derivatives, TM6008 and TM6089, exhibited strong HIF-stimulating activities (Figure 1). TM6008 is 6-amino-1, 3-di methyl-5-(2-pyridin-2-yl-quinoline-4-carbonyl)-1H-pyrimidine-2, 4-dione, and TM6089 is 6-amino-1,3-di-methyl-5-[2-(pyridin-2-ylsulfanyl)-acetyl]-1H-pyrimidine-2,4-dione.

PHD Inhibition

The inhibitory effect of our compounds on the oxygen-dependent hydroxylation of HIF-α subunit by PHD was evaluated. All tested compounds inhibited PHD activity in a dose-dependent manner (Figure 2). TM6008 was the most effective, exceeding cobalt chloride.

In Vitro Transition Metal Chelation of PHD Inhibitors

Previously reported PHD inhibitors, such as 3,4-DHB,[29] S956711,[29] and FG-0041,[27] share an iron chelating motif. Although chemical structures of TM6008 and TM6089 differ significantly from previous PHD inhibitors, TM6008 also share this motif. By contrast, TM6089 lacks this motif.

We therefore evaluated their abilities to chelate transition metals in vitro by copper-catalyzed oxidation of ascorbic acid. 3,4-DHB, S965711, and TM6008 chelated transition

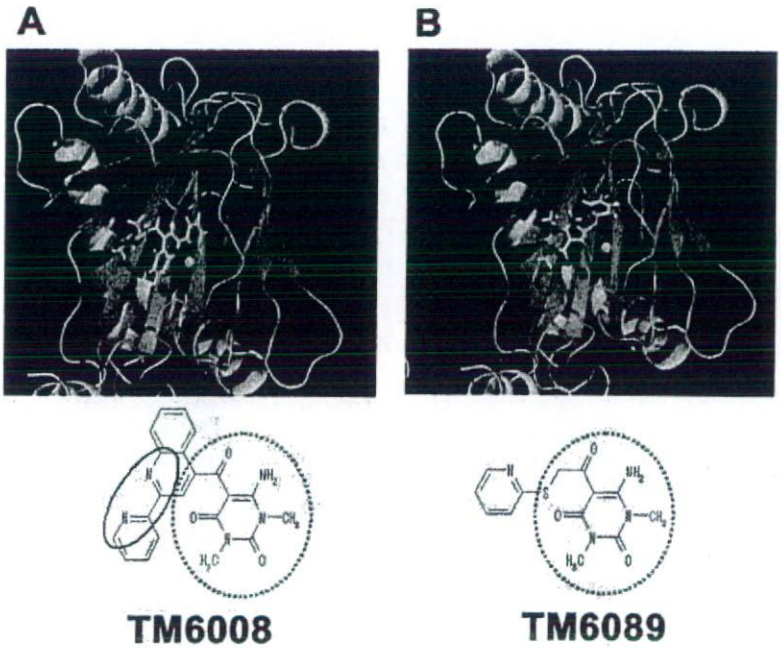

Figure 3. The predicted binding modes of TM6008 (A) and TM6089 (B) in PHD2. TM6008 and TM6089 are drawn by stick models. Sulfur, oxygen, nitrogen, carbon, and hydrogen atoms are shown in orange, red, blue, green, and white, respectively. Fe(II) is shown by an orange sphere. Figures were drawn by the software PyMOL version 0.97 (DeLano Scientific LLC).

metal (copper) and inhibited the autoxidation of ascorbic acid in a dose-dependent manner (IC 50 values were 330, 31.4, and 0.57 μmol/L, respectively). By contrast, TM6089 did not chelate transition metal even at the concentration of 100 μmol/L.

Binding Mode to Human PHD

PHD produces trans-4-hydroxyproline from 2-OG and L-proline (Pro) in the presence of Fe(II). The crystal structure of the catalytic domain of human PHD2, an important prolyl-4-hydroxylase in the human hypoxia response in normal cells, has been recently reported.[30] Based on the 3-dimensional structure of this PHD, we undertook docking simulations between our 2 PHD inhibitors and human PHD2. The docking modes of TM6008 and TM6089 are shown in Figure 3. TM6008 binds to the active site of PHD2 by chelating 2 nitrogen atoms with the iron atom. By contrast, TM6089 binds to the active site by nonchelating mechanism. The sulfur and 1 carbonyl oxygen atom of TM6089 point to the iron atom. The disposition of these 3 atoms, however, is unfavorable to form coordinate bonds. The binding mode of TM6089 demonstrates that TM6089 is a unique inhibitor without iron chelating affinity.

Toxicity and Pharmacokinetics

TM6008 and TM6089 did not exhibit cytotoxicity at the tested concentrations (up to 100 μmol/L). No acute toxicity was observed in mice up to 2 weeks after a single oral dose of 2000 mg/kg for TM6008, whereas the 50% lethal dose of TM6089 was 500 mg/kg. Pharmacokinetics studies in rats given an oral dose of 50 mg/kg of each compound disclosed plasma Tmax, Cmax, and T1/2 values of 3.5 hour, 0.9 μg/mL and 1.5 hour for TM6008, and 1.0 hour, 0.5 μg/mL, and 0.6 hour for TM6089.

Demonstration of the In Vivo Effectiveness

As VEGF is regulated by the HIF-HRE system, we examined whether TM6008 and TM6089 stimulate angiogenesis.

Firstly, we examined whether local injection of our compounds stimulates angiogenesis in vivo. For this purpose, we introduced small sponges under the skin of mice and measured their hemoglobin contents and vessel numbers after 10 days to estimate the stimulation of the HIF-HRE system. Injection of TM6008 increased angiogenesis as demonstrated by an increase of the hemoglobin content, and by an increased vessel number on immunohistochemical evaluation of the sponges. TM6089 also enhanced angiogenesis in the sponge assays (Figure 4A through 4C).

To investigate whether systemic administration of TM6008 and TM6089 stimulates in vivo the HIF-HRE system in various organs, we used the hypoxia-sensing transgenic rats. In the kidney expression of the reporter gene was not detected under basal conditions (amplification of 40 cycles), but expression of the reporter gene was obviously induced after a single oral dose 100 mg/kg of TM6008 and TM6089 (detected at 31.0±0.85 cycles and 31.0±2.05 cycles, respectively). In the liver, expression of the reporter gene, which was undetectable under basal conditions, was also induced after TM6008 administration (detected at 32.3±0.35 cycles), whereas TM6089 was ineffective. In the heart, the reporter gene was detected under basal conditions and both TM6008 and TM6089 increased its expression (1.37±1.00 and 6.69±5.45 fold increase, respectively). No attempt was made to evaluate the expression of the transgene in the brain because the pharmacokinetics studies showed that neither of the tested compounds crossed the blood-brain barrier.

Next, we evaluated capillary network formation by Matrigel assays. When endothelial cells were seeded onto Matrigel at subconfluent density, they developed tube-like structures at 9 hours. Quantification of capillary network formation by measuring the tube length revealed promotion of capillary network formation by TM6008, confirming the results of the sponge assays (Figure 4D).

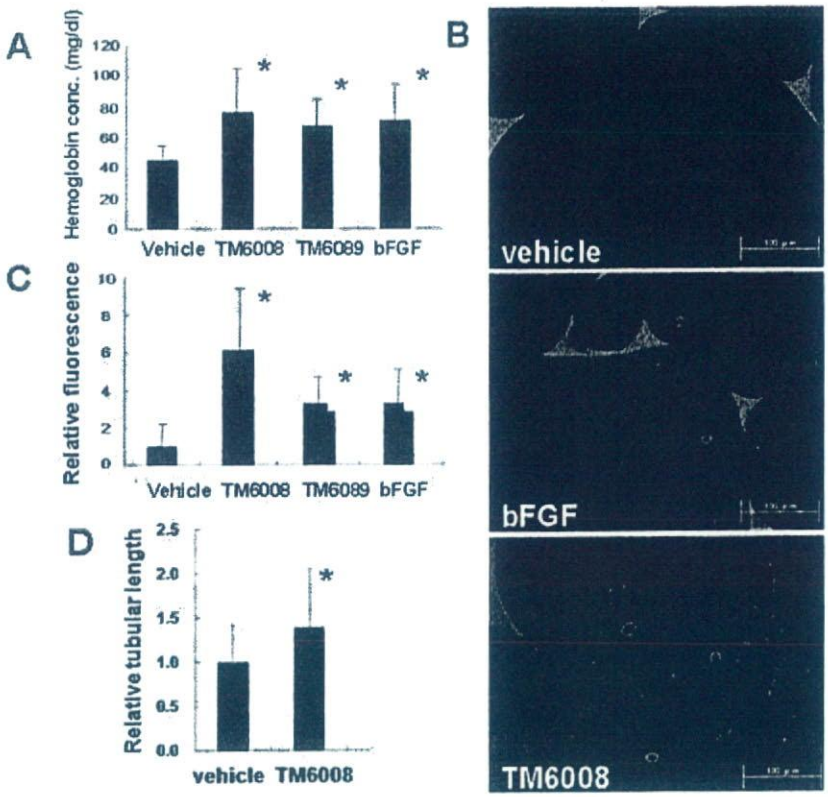

Figure 4. Stimulation of angiogenesis in the mouse sponge model and in the Matrigel assay. To assess the degree of angiogenesis, we measured the hemoglobin content in the sponge (A) and stained for the endothelial cell marker CD31 (B and C). B, Representative immunostaining of CD31 (×200); C, The average number of vessels. D, Capillary network formation on the Matrigel. *$P<0.05$ vs vehicle.

Prevention of Neuronal Cell Death Induced by Hypoxia

PHD inhibitors might protect cells against hypoxic damage. To test this hypothesis we used the delayed neuronal death model in gerbil. Nontoxic TM6008 (100 mg/kg/d) was given orally for 7 days in gerbils after a 5-minute transient global cerebral ischemia. The pathological outcome of neuronal cells was examined after 7 day administration of TM6008 in CA1 hippocampus with light microscopy.

In contrast with nonischemic gerbils (Figure 5A), gerbils subjected to ischemia and given vehicle alone (Figure 5B) exhibited in most pyramidal neurons ischemic cell damage, characterized by shrunken, darkly stained cytoplasm, and pyknotic nuclei with accumulation of glial cells. In the TM6008-treated animals, only a few neurons showed ischemic changes (Figure 5C). The number of viable neurons in the CA1 hippocampus, was higher in the TM6008-treated animals than in the vehicle-treated gerbils (166±73 versus

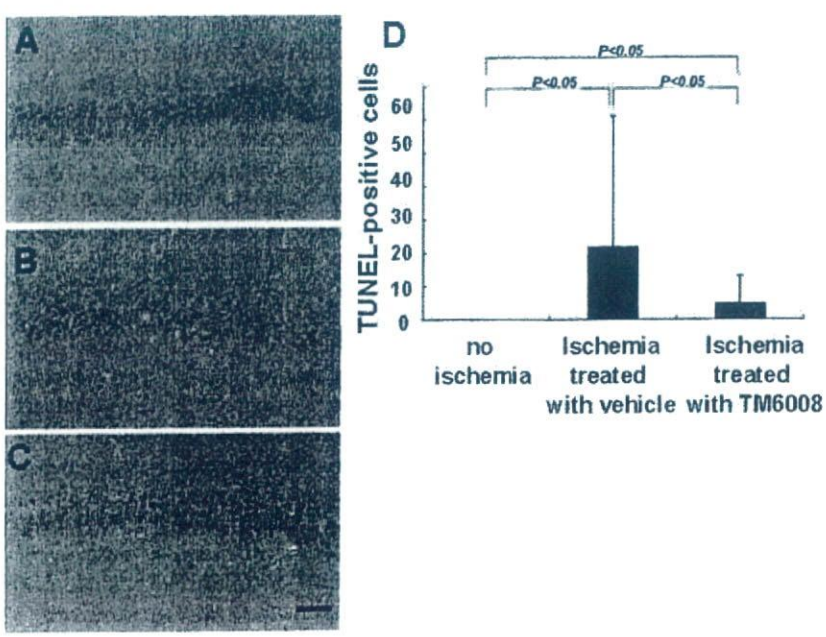

Figure 5. Prevention of hypoxic-induced neuronal cell death. HE staining in CA1 in a nonischemia animal (A), an animal subjected to ischemia and treated with vehicle alone (B), and an animal subjected to ischemia and treated with TM6008 (C). Scale bar=0.1 mm. D, TUNEL-positive cells in CA1.

61±55, $P<0.05$). The number of viable neurons in the CA1 hippocampus of the TM6008-treated animals was not statistically different from that observed in the nonischemia control group (227±50). Further, treatment with TM6008 decreased the number of apoptotic cells (Figure 5D). The final plasma concentration of TM6008 in these experiments was 7.8±2.9 μg/mL. Thus, TM6008 clearly protected against hypoxia-induced apoptotic neuronal death.

Next, we examined whether the protective effect of TM6008 against delayed neuronal death was attributable to enhanced angiogenesis. There was no statistically significant difference of the number of VEGF-positive cells between TM6008- and vehicle-treated groups (10.17±5.02 versus 9.12±1.55, respectively). Further, there was no significant difference of the value of cortical microperfusion at 7 days after occlusion between TM6008- and vehicle-treated groups (25.0±9.3 versus 29.4±8.7, respectively).

To clarify a neuroprotective mechanism of TM6008 in global ischemia models, we immunohistochemically stained with EPO, GLUT-1, and GLUT-3. The number of GLUT-3–positive cells in the CA1 hippocampus was significantly higher in TM6008 treated than in the vehicle-treated gerbils (26.9±7.5 versus 15.3±8.6, $P<0.05$). However, there was no statistically significant difference in EPO or GLUT-1–positive cells in the CA1 hippocampus between TM6008- and vehicle-treated groups (2.9±2.9 versus 3.3±1.7; and 5.5±2.1 versus 6.4±1.8, respectively).

Discussion

We identified novel molecules able to inhibit PHD activity and stabilize HIF. Our docking simulation studies based on the 3 dimensional structure of PHD2 have disclosed the molecular events required to inhibit PHD and therefore stabilize HIF. The target of these PHD inhibitors is the PHD active site.

Most of the PHD inhibitors reported so far, eg, 3,4-DHB, S956711 and FG-0041, are believed to inhibit the enzyme by iron chelating mechanism.[27,29] Iron chelating compounds could have nonspecific binding affinity to the iron containing proteins or iron ions and may not be desirable from the therapeutic point of view because iron is an essential cofactor for a host of important cellular functions, including oxidative phosphorylation and arachidonic acid signaling. To our surprise, the docking simulations demonstrated that TM6089 could preferentially bind to the active site of PHD2 without chelating to the iron atom. Indeed, TM6089 is devoid of iron chelating activity in vitro. Thus, iron chelation is not a necessary intermediate of PHD inhibition. According to our knowledge, TM6089 is the first unique PHD inhibitor which stimulates HIF activity without iron chelation.

The in vivo relevance of our novel PHD inhibitors was first demonstrated by the sponge assay in mice. Previous reports have shown that the hemoglobin contents of the sponge implants and the surrounding granuloma tissue correlated with the degree of angiogenesis.[31] Accordingly, both 3,4-DHB and S956711 were shown to raise the number of vessels in the sponge. In this study, we demonstrated not only an augmented number of vessels by immunohistochemistry but also an increased hemoglobin content in the sponge after local administration of TM6008 and TM6089.

Of great interest, these effects of TM6008 and TM6089 are not restricted locally but extend to several organs. To reach this conclusion, we used a hypoxia-sensing transgenic rat expressing a hypoxia-responsive reporter vector using a HRE of the 5′ VEGF untranslated region.[25] These transgenic rats have the unique asset to allow a sensitive and specific evaluation of HIF stimulation. As a consequence of systemic administration of TM6008 and TM6089 to these rats, expression of the reporter gene was considerably upregulated in the kidney, liver, and heart.

To extend these findings, we used less toxic TM6008 and obtained therapeutically relevant results in studies using gerbils. In gerbils, transient brain ischemia followed by reperfusion results in neuronal death in selectively vulnerable brain regions such as the hippocampal CA1 sector and caudate-putamen. The discovery that, in this model, TM6008 rescued neurons from apoptotic cell death in the CA1 hippocampus is noteworthy. Whereas TM6008 did not cross the blood-brain barrier, TM6008 protected the brain in a model of global cerebral ischemia. This is likely attributable to an increase in permeability of the blood-brain barrier, as previous reports showed that ischemic injury in this model destroys the blood-brain barrier and allows passage of compounds which do not penetrate the barrier under normal conditions.[32]

Mechanisms of neuroprotection by TM6008 can theoretically be multifactorial because HIF regulates a wide range of protective genes such as those involved in erythropoiesis (EPO, transferring, and hepcidin), angiogensis (VEGF), antioxidative stress (HO-1), glycolysis (Glut-1, Glut-3, and aldolase A), and so on. Angiogenic effects of TM6008 shown by the Matrigel assays and sponge assays stimulated us to study whether enhanced angiogenesis played a role in neuronal protection in our model. However, we could not find enhanced angiogenesis in the brain of gerbils treated with TM6008 by counting VEGF-positive vessels or measuring blood flow by laser Doppler flowmetry. Therefore, it is unlikely that the protective effect of TM6008 was related to angiogenesis in the gerbil forebrain ischemia model. This may be explained by different concentrations of TM6008 among the assays. Although we could not measure the local concentrations of TM6008 in the damaged brain, it is likely that the concentration of the gerbil forebrain treated with TM6008 p.o. is lower than those obtained by local administration such as sponge assays and Matrigel assay.

We next focused on effects of TM6008 on neuronal apoptosis. Our terminal deoxynucleotidyl transferase-mediated dUTP nick end-labeling (TUNEL) assays demonstrated that TM6008 decreased the number of apoptotic cells in the brain, and other potential neuroprotective mechanisms by TM6008 include antiapoptotic effects mediated by other HIF-regulated genes such as EPO,[33] VEGF,[34] and glucose transporters.[35] EPO is a pleiotropic cytokine[36] and induces neuroprotection via the antiapoptotic signaling cascades like Bcl-X_L through direct binding to the Bcl-X promoter.[37] Antiapoptotic effects of VEGF contribute to reduction of ischemic brain damage in addition to its angiogenic effects.[38]